

## Examination of Acylated 4-Aminopiperidine-4-carboxylic Acid Residues in the Phosphotyrosyl+1 Position of Grb2 SH2 Domain-Binding Tripeptides

Sang-Uk Kang,<sup>†</sup> Won Jun Choi,<sup>†</sup> Shinya Oishi,<sup>†</sup> Kyeong Lee,<sup>†</sup> Rajeshri G. Karki,<sup>†</sup> Karen M. Worthy,<sup>‡</sup> Lakshman K. Bindu,<sup>‡</sup> Marc C. Nicklaus,<sup>†</sup> Robert J. Fisher,<sup>‡</sup> and Terrence R. Burke, Jr.\*<sup>†</sup>

Laboratory of Medicinal Chemistry, Center for Cancer Research, National Cancer Institute, National Institutes of Health, Frederick, Maryland 21702, Protein Chemistry Laboratory, Science Applications International Corporation-Frederick, Frederick, Maryland 21702

Received December 7, 2006

A 4-aminopiperidine-4-carboxylic acid residue was placed in the pTyr+1 position of a Grb2 SH2 domain-binding peptide to form a general platform, which was then acylated with a variety of groups to yield a library of compounds designed to explore potential binding interactions, with protein features lying below the  $\beta$ D strand. The highest affinities were obtained using phenylethyl carbamate and phenylbutyrylamide functionalities.

### Introduction

Significant research has been devoted to enhancing binding affinity, cellular potency, and metabolic stability of Grb2 SH2 domain binding antagonists.<sup>1</sup> These efforts have included the use of bend-inducing 1-aminocyclohexanecarboxylic acid (Ac<sub>6</sub>c<sup>d</sup>) residues in the pTyr+1 position of “pTyr–Xxx–Asn”-containing peptides.<sup>2</sup> However, little has been reported regarding potential binding interactions that might result by extending functionality outward from the Ac<sub>6</sub>c side chain ring.<sup>3</sup> Residues Val99, Phe101, Gln106, Phe108, Ser141, Asn143, and Gln144 of the Grb2 SH2 domain lie along and below the protein  $\beta$ D strand (nomenclature based on structural homology among SH2 domains).<sup>4</sup> These residues form a region proximal to the pTyr+1 position that could potentially interact with functionality derived from suitably modified Ac<sub>6</sub>c residues. Starting from a previously reported Ac<sub>6</sub>c-containing tripeptide inhibitor,<sup>5</sup> replacement of the Ac<sub>6</sub>c residue with 4-aminopiperidine-4-carboxylic acid (Apc)<sup>6</sup> and elaboration at the piperidinyl 1-position would yield analogues of type **8** (Scheme 1) that could potentially interact with this region of the protein.

To explore these potential interactions, preparation of a small library of Apc-containing final products (**8**) was accomplished using the known intermediates **1**,<sup>7</sup> **2**,<sup>8</sup> and **4**,<sup>5</sup> as shown in Scheme 1. Of note, coupling **3** with the protected pTyr mimetic **4** required HOAt (1-hydroxy-7-azabenzotriazole) active ester methodology due to steric hindrance.<sup>5</sup> Hydrogenolytic cleavage of the Apc 1-amino-Cbz group in **5** gave the free piperidino-containing analogue **6**, which upon acylation, yielded the series of analogues **7**. The products **7a–d** and **7j** were prepared using chloroformates, while HOBt active ester coupling was employed for compound **7e**, and acid chlorides were used for **7f**, **7g**, and **7i**. The synthesis of urea **7h** employed an isocyanate. Treatment of the *tert*-butyl-protected products **7** with TFA gave the final products **8a–j**, which were purified by HPLC.

### Evaluation of Inhibitors in a Grb2 SH2 Domain-Binding System

Kinetic binding data for peptides **8a–j** were obtained by surface plasmon resonance experiments that measured the direct interaction of synthetic ligands with surface-bound Grb2 SH2 domain protein (Table 1).<sup>9</sup> The pTyr+1 Ac<sub>6</sub>c-containing peptide has a reported Grb2 SH2 domain-binding affinity of 24 nM.<sup>3</sup> Methyl carbamate **8a** represents the simplest analogue examined in the current study and its binding affinity ( $K_D = 106$  nM) serves as a reference for comparison with the remainder of the series. Elaboration of the methyl carbamate to a 2-methoxyethyl carbamate (**8b**,  $K_D = 202$  nM) resulted in a loss of affinity, and introduction of an aromatic group resulted in further loss of affinity when a one-methylene spacer was employed (benzyl carbamate **8c**,  $K_D = 320$  nM). However, adding an additional methylene group to **8c** increased affinity 10-fold (phenylethyl carbamate **8d**,  $K_D = 35.7$  nM). Molecular modeling simulations were performed on compounds **8a**, **8c**, and **8d** bound to the Grb2 SH2 domain protein with the Insight II2000.0/Discover 97.0 modeling package (Molecular Simulations, Inc., San Diego, CA) using the cff91 force field. When the crystal structure of mAZ-pY-( $\alpha$ Me)pY-N–NH<sub>2</sub> bound to the Grb2 SH2 domain (1JYQ.pdb) was used, the peptide ligand was modified using 3D-sketcher tools to yield inhibitors **8a**, **8c**, **8d**, and **8j**, and these were subjected to energy minimization and molecular dynamics simulations (see the Supporting Information). It was found that **8d** exhibited the best extension within the target region below the  $\beta$ D strand (Figure 1).

Replacement of the carbamoyl oxygen of **8d** with a methylene yielded the corresponding phenylbutyrylamide **8e** ( $K_D = 27$  nM). Addition of one methylene to **8e** gave the phenylvaleramide **8f**, which suffered a significant loss of binding affinity ( $K_D = 2180$  nM). This indicated that a chain extension of 3 units beyond the carbonyl was preferable to 4 units. Accordingly, the indole-containing analogue **8g** was prepared to present a 3-unit extension between the phenyl ring and the amide carbonyl (the indolyl nitrogen is considered as part of the extending chain). Likewise, analogue **8h** was prepared as a urea variant of carbamate **8d**. The affinities of **8g** ( $K_D = 458$  nM) and **8h** ( $K_D = 272$  nM) were less than **8d**, as was the affinity of sulfonamide **8i** ( $K_D = 2140$  nM).

The analogue **8j** contains a 4-carboxybenzyl carbamate moiety. Previous work has shown that pTyr or pTyr mimetics placed at the pTyr+1 position can promote high affinity binding by interacting with the Grb2 SH2 domain Arg142 residue.<sup>3,10</sup>

\* To whom correspondence should be addressed. Laboratory of Medicinal Chemistry, Center for Cancer Research, National Cancer Institute, National Institutes of Health, NCI-Frederick, P.O. Box B, Bldg. 376 Boyles St., Frederick, Maryland 21702-1201. Tel.: (301) 846-5906. Fax: (301) 846-6033. E-mail: tburke@helix.nih.gov.

<sup>†</sup> Center for Cancer Research.

<sup>‡</sup> Science Applications International Corporation.

<sup>d</sup> Abbreviations: pTyr, phosphotyrosyl; Ac<sub>6</sub>c, aminocyclohexanecarboxylic acid; Apc, 4-aminopiperidine-4-carboxylic acid; HOAt, 1-hydroxy-7-azabenzotriazole.

Scheme 1. Synthesis of Analogues Used in the Current Study

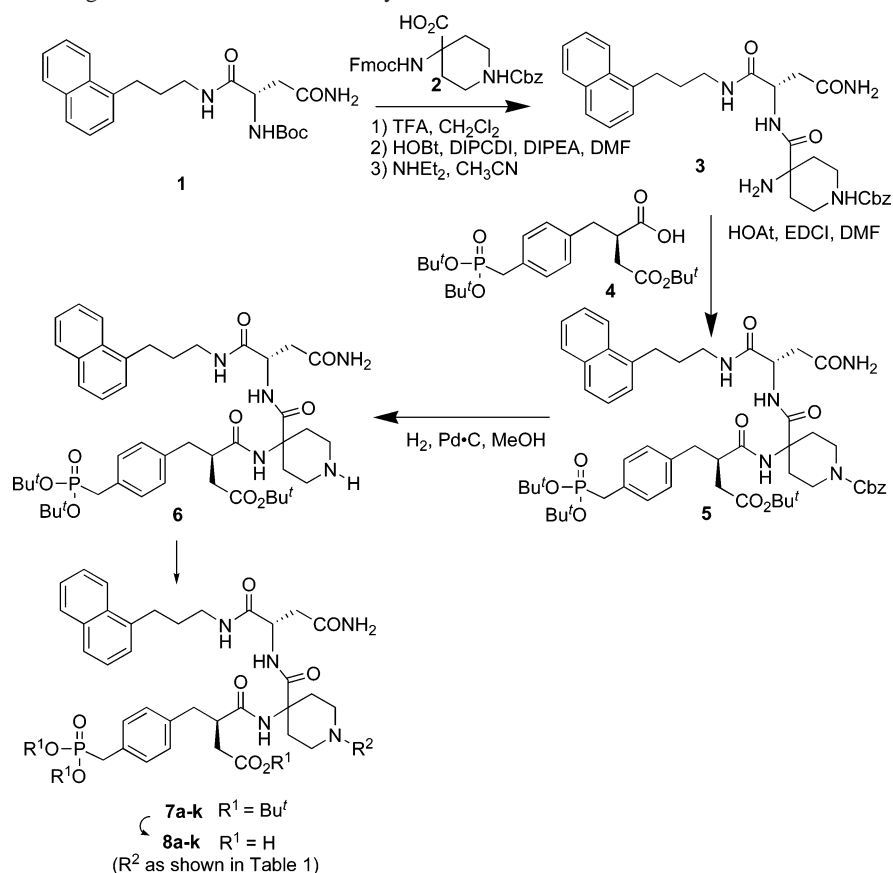


Table 1. Grb2 SH2 Domain-Binding Affinities of Synthetic Inhibitors Determined by Surface Plasmon Resonance

No.	R <sup>2a</sup>	K <sub>D</sub> (nM) <sup>b</sup>	No.	R <sup>2a</sup>	K <sub>D</sub> (nM) <sup>b</sup>
8a		106	8f		2180
8b		202	8g		458
8c		320	8h		272
8d		36	8i		2140
8e		27	8j		871

<sup>a</sup> Placement of R groups is as shown in Scheme 1. <sup>b</sup> Data was obtained by surface plasmon resonance experiments as described in the Supporting Information.<sup>9</sup>

Although the structure of the 4-carboxybenzyl carbamoyl moiety represents a departure from the more traditional pTyr mimetics used in these prior studies, modeling studies showed that interaction of the 4-carboxybenzyl group with the Arg142 residue was possible (Figure 1D). However, the poor affinity of **8j** ( $K_D = 871$  nM) indicated that the desired interaction of the 4-carboxybenzyl group with the Arg142 residue was not achieved.

**Conformationally-Constrained Amide Surrogates.** The phenylbutyrylamide side chain of the most potent analogue **8e** could potentially bind in two distinct conformations due to rotational restriction about the amide C(=O)-N bond. This type of rotamer would not be expected for the carbamoyl linkage in the homologous structure **8d**. As one approach toward examining whether rotamers about the phenylbutyrylamide bond at the Apc 4-position might contribute differently to the affinity

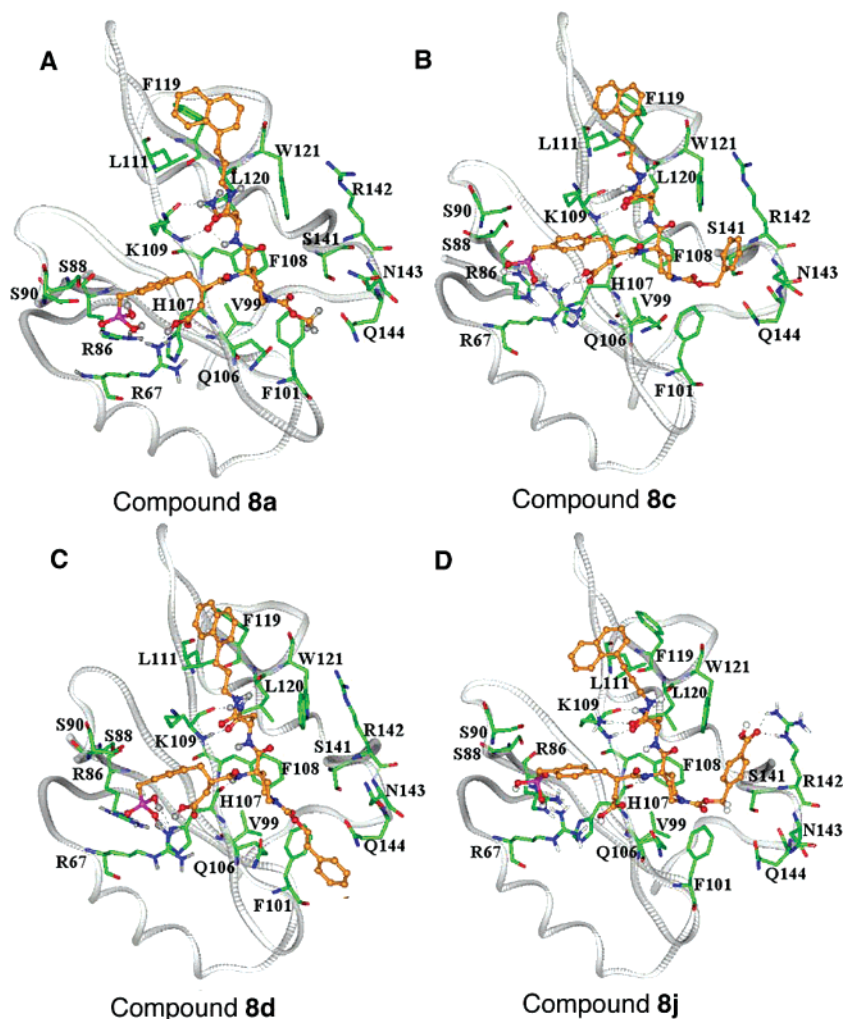


**Figure 1.** Structures of analogues **8a**, **8c**, **8d**, and **8j** (in gold) docked into the Grb2 SH2 domain. The protein is shown in ribbon depiction, with important side chain groups shown in ball and stick rendering.

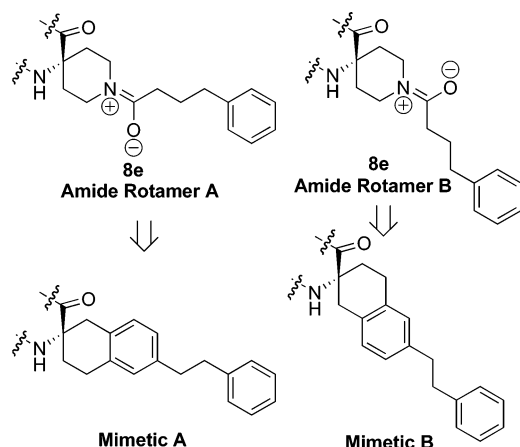


**Figure 2.** Use of pTyr+1 2-amino-2-carboxytetralin-based residues as conformationally constrained mimetics of amide rotamers arising from the phenylbutyrylamide of **8e**.

of compound **8e**, the tetralin-based analogues “mimetic A” and “mimetic B” were designed as conformationally constrained amide replacements (Figure 2).<sup>11</sup> However, the low affinity of both mimetic A and mimetic B ( $K_D$  values  $> 10 \mu\text{M}$ ) indicated that the tetralin platforms lacked critical functionality needed to function as conformationally constrained amide bond surrogates.

Binding affinities alone may not reflect subtle differences in binding kinetics, because similar  $K_D$  values may arise from markedly different rates of association and dissociation. Interaction kinetic maps that plot association rates ( $k_a$ ) versus dissociation rates ( $k_d$ ), with an overlay of  $K_D$  isovalues, can allow visual discrimination of classes of compounds based on similar binding behaviors.<sup>12</sup> Plotting **8a–j** in this fashion indicated three groups of compounds (Figure 3): Group A compounds (**8d** and **8e**) display slow dissociate rates and relatively higher association rates. Although conversion of the carbamate functionality of **8d** into the amide group of **8e** introduced significant changes in rotational flexibility and hydrogen-bonding potential, little difference was observed in the actual binding affinities of **8d** and **8e**. Instead, the structural change resulted in a marked decrease in the rate of dissociation for **8e**. This may mean that **8e** is a more desirable inhibitor than **8d**, because low dissociation rates have been hypothesized to enhance the efficacy of drug-target interactions.<sup>12</sup> The Group B compound (**8a**) exhibits a higher association rate, but this is also accompanied by a more rapid dissociation rate. Group C compounds (**8b**, **8c**, and **8f–j**) exhibit slower association rates as well as moderate to rapid dissociation rates.

## Conclusions

When a 4-piperidinyI variant of the known pTyr+1 residue Ac<sub>6</sub>c was used, the current study investigated the effects of extending functionality outward from the Ac<sub>6</sub>c residue to take

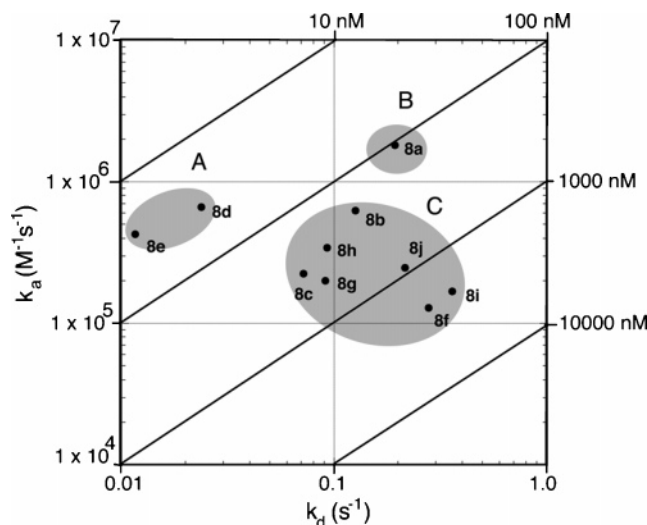


**Figure 3.** Interaction kinetic maps for Grb2 SH2 domain-binding inhibitors **8a–e** plotting association rate ( $k_a$ ) versus dissociation rate ( $k_d$ ) with an overlay of  $K_D$  isovalues. Data was organized into three groups, A, B, and C, depending on a combination of these factors.

advantage of potential interactions with an unexplored region of the Grb2 protein lying beneath the  $\beta D$  strand. Carbamoyl, amido, urea, and sulfonamido linkages to the 4-piperidinyl nitrogen were prepared. Tethering phenyl rings at varying distances from the piperidinyl nitrogen indicated that the best affinities were provided by a three-unit chain, with a phenylbutyryl amide group provided the highest affinity. Because SH2 domains share a high degree of structural homology, the current approach may be useful in preparing binding inhibitors directed at other SH2 domains.

## Experimental Section

**Synthesis of Dipeptide 3.** Reacting **1**<sup>7</sup> and commercially available *N*<sup>α</sup>-Fmoc-(4-*N*-Cbz-piperidinyl)carboxylic acid<sup>8</sup> according to protocols similar to those reported for the synthesis of the corresponding Ac<sub>6</sub>C-containing congener, the dipeptide **3** was obtained in 89% yield as a white solid (mp 169–171 °C). <sup>1</sup>H NMR (DMSO-*d*<sub>6</sub>)  $\delta$  8.43 (1H, s), 8.06 (1H, d,  $J$  = 8.4 Hz), 7.90 (1H, m), 7.83 (1H, t,  $J$  = 5.5 Hz), 7.75 (1H, d,  $J$  = 7.8 Hz), 7.56–7.47 (2H, m), 7.43–7.29 (2H, m), 6.87 (1H, s), 5.07 (2H, s), 4.46 (1H, m), 3.75 (2H, m), 3.21–3.10 (4H, m), 3.02 (2H, t,  $J$  = 7.6 Hz), 2.57–2.42 (2H, m), 1.91–1.73 (4H, m), 1.33 (2H, t,  $J$  = 14.3 Hz). FAB-MS (+VE)  $m/z$  560 (MH<sup>+</sup>).

**Synthesis of Protected Tripeptide Mimetic 5.** Similar to a previously reported procedure,<sup>5</sup> to a solution of dipeptide **3** (784 mg, 1.40 mmol) in DMF (2 mL) was added an active ester solution formed by reacting **4**<sup>5</sup> (988 mg, 2.10 mmol), HOAt (0.5 M in DMF, 4.20 mL, 2.10 mmol), and EDCI·HCl (425 mg, 3.36 mmol) in DMF (3 mL; 15 min at room temperature), and the mixture was stirred at 40 °C (21 h). Solvent was removed by vacuum distillation, and the remaining residue was purified by silica gel column chromatography to provide **5** as a white solid (835 mg, 59% yield), mp 153–155 °C. <sup>1</sup>H NMR (CDCl<sub>3</sub>)  $\delta$  8.06 (1H, d,  $J$  = 8.0 Hz), 7.88 (1H, d,  $J$  = 7.8 Hz), 7.82 (1H, m), 7.68 (1H, dd,  $J$  = 3.1 and 6.4 Hz), 7.49–7.40 (3H, m), 7.37–7.29 (6H, m), 7.19–7.09 (3H, m), 6.99 (2H, d,  $J$  = 7.8 Hz), 6.92 (1H, s), 6.46 (1H, s), 5.49 (1H, s), 5.10 (2H, s), 4.60 (1H, s), 3.92 (2H, m), 3.35 (2H, m), 3.12 (2H, m), 3.04–2.88 (7H, m), 2.66 (1H, m), 2.49 (2H, m), 2.25 (1H, m), 2.13–1.80 (6H, m), 1.41 (9H, s), 1.39 (9H, s), 1.34 (9H, s). FAB-MS (+VE)  $m/z$  1012 (MH<sup>+</sup>).

**General Procedures for the Synthesis of Final Products 8a–8j.** Protected tripeptide mimetic **5** in MeOH was hydrogenated over 10% Pd·C (50% by weight of **5**) using a balloon filled with H<sub>2</sub> gas (overnight). The reaction mixture was filtered and taken to dryness then dissolved in CH<sub>2</sub>Cl<sub>2</sub> to provide a 0.1 M stock solution of free

amine **6**. Aliquots of the stock solution were reacted with appropriate acylating agents in the presence of diisopropylethylamine to yield protected intermediates **7a–j**. Yields and spectral data are provided as Supporting Information. For intermediates **7a–d** and **7j**, acylations were performed using chloroformates, while HOBT active ester coupling was employed for intermediate **7e**, and acid chlorides were used for **7f**, **7g**, and **7i**. The synthesis of urea **7h** employed the appropriate isocyanate. Treatment of the *tert*-butyl-protected products **7** with a mixture of TFA/H<sub>2</sub>O/ethanedithiol (3:0.1:0.1) gave the globally deprotected final products **8a–j**. Physical data and combined yields from **6** following HPLC purification are provided below.

**Final Product 8a:** 64% yield; <sup>1</sup>H NMR (DMSO-*d*<sub>6</sub>)  $\delta$  8.62 (1H, s), 8.11 (1H, m), 7.99 (1H, d,  $J$  = 8.2 Hz), 7.92 (1H, m), 7.77 (1H, t,  $J$  = 4.7 Hz), 7.53–7.49 (2H, m), 7.46–7.39 (4H, m), 7.13–7.11 (2H, m), 6.96–6.93 (3H, m), 4.35 (1H, m), 3.68 (2H, m), 3.59 (3H, s), 3.25–3.02 (7H, m), 2.89 (2H, d,  $J$  = 21.3 Hz), 2.71 (1H, dd,  $J$  = 6.4 and 14.6 Hz), 2.53–2.42 (2H, m), 2.33 (1H, m), 2.01–1.66 (8H, m). FAB-MS (–VE)  $m/z$  766 (M – H). HRMALDI-MS (+VE) calcd for C<sub>37</sub>H<sub>46</sub>N<sub>5</sub>O<sub>11</sub>NaP [M + Na], 790.2824; found, 790.2787.

**Final Product 8b:** 52% yield; <sup>1</sup>H NMR (DMSO-*d*<sub>6</sub>)  $\delta$  8.63 (1H, s), 8.11 (1H, d,  $J$  = 7.6 Hz), 8.00 (1H, d,  $J$  = 8.2 Hz), 7.92 (1H, m), 7.78 (1H, t,  $J$  = 4.7 Hz), 7.54–7.41 (6H, m), 7.12 (2H, m), 6.95 (3H, m), 4.36 (1H, m), 4.11 (2H, m), 3.69 (2H, m), 3.51 (2H, t,  $J$  = 4.5 Hz), 3.26 (3H, s), 3.26–3.00 (7H, m), 2.89 (2H, d,  $J$  = 21.5 Hz), 2.71 (1H, dd,  $J$  = 6.4 and 15.8 Hz), 2.54–2.43 (2H, m), 2.33 (1H, m), 2.01–1.70 (8H, m). FAB-MS (–VE)  $m/z$  810 (M – H). HRMALDI-MS (+VE) calcd for C<sub>39</sub>H<sub>50</sub>N<sub>5</sub>O<sub>12</sub>NaP [M + Na], 834.3121; found, 834.3086.

**Final Product 8c:** 76% yield; <sup>1</sup>H NMR (DMSO-*d*<sub>6</sub>)  $\delta$  8.64 (1H, s), 8.11 (1H, m), 8.00 (1H, d,  $J$  = 8.2 Hz), 7.91 (1H, m), 7.77 (1H, t,  $J$  = 4.9 Hz), 7.54–7.30 (11H, m), 7.12 (2H, m), 6.94 (3H, m), 5.08 (2H, s), 4.35 (1H, m), 3.73 (2H, m), 3.24–2.91 (7H, m), 2.89 (2H, d,  $J$  = 21.3 Hz), 2.70 (1H, dd,  $J$  = 6.8 and 15.8 Hz), 2.53–2.43 (2H, m), 2.33 (1H, m), 2.01–1.70 (8H, m). FAB-MS (–VE)  $m/z$  842 (M – H). HRMALDI-MS (+VE) calcd for C<sub>43</sub>H<sub>20</sub>N<sub>5</sub>O<sub>11</sub>NaP [M + Na], 866.3137; found, 866.3101.

**Final Product 8d:** 65% yield; <sup>1</sup>H NMR (DMSO-*d*<sub>6</sub>)  $\delta$  8.61 (1H, s), 8.11 (1H, m), 7.99 (1H, d,  $J$  = 8.0 Hz), 7.92 (1H, m), 7.77 (1H, t,  $J$  = 4.5 Hz), 7.53–7.48 (2H, m), 7.46–7.39 (4H, m), 7.31–7.19 (5H, m), 7.11 (2H, m), 6.95 (3H, m), 4.35 (1H, m), 4.17 (2H, m), 3.66 (2H, m), 3.25–3.00 (7H, m), 2.91–2.86 (4H, m), 2.71 (1H, dd,  $J$  = 6.3 and 15.6 Hz), 2.54–2.42 (2H, m), 2.33 (1H, m), 1.99 (1H, m), 1.92–1.78 (6H, m), 1.67 (1H, m). FAB-MS (–VE)  $m/z$  856 (M – H). HRMALDI-MS (+VE) calcd for C<sub>44</sub>H<sub>52</sub>N<sub>5</sub>O<sub>11</sub>NaP [M + Na], 880.3293; found, 880.3261.

**Final Product 8e:** 65% yield; <sup>1</sup>H NMR (DMSO-*d*<sub>6</sub>)  $\delta$  8.65 (1H, d,  $J$  = 13.3 Hz), 8.11 (1H, m), 8.00 (1H, t,  $J$  = 8.8 Hz), 7.92 (1H, m), 7.78 (1H, t,  $J$  = 4.9 Hz), 7.55–7.39 (6H, m), 7.28 (2H, m), 7.19–7.11 (5H, m), 6.98–6.92 (3H, m), 4.35 (1H, m), 4.05 (1H, m), 3.56 (1H, m), 3.27–2.68 (11H, m), 3.20–2.24 (4H, m), 2.40–2.22 (3H, m), 2.05–1.61 (9H, m). HRMALDI-MS (+VE) calcd for C<sub>45</sub>H<sub>54</sub>N<sub>5</sub>O<sub>10</sub>NaP [M + Na], 878.3501; found, 878.3513.

**Final Product 8f:** 60% yield; <sup>1</sup>H NMR (DMSO-*d*<sub>6</sub>)  $\delta$  8.64 (1H, d,  $J$  = 8.2 Hz), 8.11 (1H, d,  $J$  = 8.0 Hz), 8.00 (1H, t,  $J$  = 7.0 Hz), 7.91 (1H, m), 7.77 (1H, t,  $J$  = 4.9 Hz), 7.55–7.39 (6H, m), 7.27 (2H, m), 7.16 (5H, m), 6.96 (3H, m), 4.35 (1H, m), 4.03 (1H, m), 3.61 (1H, m), 3.27–2.97 (7H, m), 2.89 (2H, d,  $J$  = 21.5 Hz), 2.82–2.68 (2H, m), 2.60–2.29 (8H, m), 2.04–1.75 (6H, m), 1.65–1.46 (4H, m). FAB-MS (–VE)  $m/z$  868 (M – H). HRMALDI-MS (+VE) calcd for C<sub>46</sub>H<sub>56</sub>N<sub>5</sub>O<sub>10</sub>NaP [M + Na], 892.3657; found, 892.3697.

**Final Product 8g:** 57% yield; <sup>1</sup>H NMR (DMSO-*d*<sub>6</sub>)  $\delta$  8.64 (1H, s), 8.10 (1H, d,  $J$  = 8.2 Hz), 7.97 (1H, d,  $J$  = 7.4 Hz), 7.90 (1H, m), 7.77 (1H, m), 7.54–7.29 (9H, m), 7.11 (2H, m), 6.94 (4H, m), 6.28 (1H, d,  $J$  = 2.5 Hz), 4.35 (3H, m), 4.05 (1H, m), 3.53 (1H, m), 3.24–2.97 (7H, m), 2.92–2.68 (5H, m), 2.53–2.43 (2H, m), 2.36 (3H, s), 2.36–2.29 (1H, m), 2.00–1.64 (8H, m). FAB-MS (–VE)  $m/z$  893 (M – H). HRMALDI-MS (+VE) calcd for C<sub>47</sub>H<sub>58</sub>N<sub>6</sub>O<sub>10</sub>NaP [M + Na], 917.3610; found, 917.3636.



**Final Product 8h:** 67% yield;  $^1\text{H NMR}$  ( $\text{DMSO}-d_6$ )  $\delta$  8.58 (1H, s), 8.12 (1H, d,  $J = 7.8$  Hz), 7.97–7.91 (2H, m), 7.78 (1H, m), 7.55–7.47 (3H, m), 7.44–7.39 (3H, m), 7.30–7.27 (2H, m), 7.18 (3H, m), 7.12 (2H, m), 6.97–6.92 (3H, m), 6.60 (1H, br s), 4.35 (1H, m), 3.64 (2H, m), 3.25–2.90 (8H, m), 2.91 (2H, d,  $J = 21.1$  Hz), 2.79–2.69 (4H, m), 2.55–2.45 (2H, m), 2.35 (1H, dd,  $J = 10.0$  and  $13.7$  Hz), 2.03–1.63 (8H, m). FAB-MS ( $-VE$ )  $m/z$  855 ( $M - H$ ). HRMALDI-MS ( $+VE$ ) calcd for  $\text{C}_{44}\text{H}_{53}\text{N}_6\text{O}_{10}\text{NaP}$  [ $M + \text{Na}$ ], 879.3453; found, 879.3416.

**Final Product 8i:** 32% yield;  $^1\text{H NMR}$  ( $\text{DMSO}-d_6$ )  $\delta$  8.61 (1H, s), 8.11 (1H, d,  $J = 7.7$  Hz), 8.02 (1H, d,  $J = 8.1$  Hz), 7.91 (1H, m), 7.77 (1H, t,  $J = 5.0$  Hz), 7.55–7.20 (11H, m), 7.10 (2H, m), 6.92 (3H, m), 4.36 (1H, m), 3.43 (2H, m), 3.30 (2H, m), 3.19 (2H, m), 3.07 (5H, m), 2.94 (2H, m), 2.88 (2H, d,  $J = 21.5$  Hz), 2.71 (1H, dd,  $J = 6.6$  and  $15.8$  Hz), 2.54–2.42 (2H, m), 2.31 (1H, m), 2.01–1.79 (8H, m). FAB-MS ( $-VE$ )  $m/z$  876 ( $M - H$ ). HRMALDI-MS ( $+VE$ ) calcd for  $\text{C}_{43}\text{H}_{52}\text{N}_5\text{O}_{11}\text{NaP}$  [ $M + \text{Na}$ ], 900.3014; found, 900.3039.

**Final Product 8j:** 55% yield;  $^1\text{H NMR}$  ( $\text{DMSO}-d_6$ )  $\delta$  8.65 (1H, s), 8.11 (1H, m), 8.01 (1H, d,  $J = 8.4$  Hz), 7.96–7.90 (3H, m), 7.77 (1H, t,  $J = 5.1$  Hz), 7.57–7.40 (8H, m), 7.12 (2H, m), 6.97–6.93 (3H, m), 5.16 (2H, s), 4.36 (1H, m), 3.75 (2H, m), 3.25–3.01 (7H, m), 2.89 (2H, d,  $J = 21.3$  Hz), 2.71 (1H, dd,  $J = 6.3$  and  $15.8$  Hz), 2.54–2.43 (2H, m), 2.33 (1H, m), 2.02–1.72 (8H, m). FAB-MS ( $-VE$ )  $m/z$  886 ( $M - H$ ). HRMALDI-MS ( $+VE$ ) calcd for  $\text{C}_{44}\text{H}_{50}\text{N}_5\text{O}_{13}\text{NaP}$  [ $M + \text{Na}$ ], 910.3035; found, 910.3006.

**Acknowledgment.** The authors wish to thank Drs. James A. Kelley and Christopher Lai of the Laboratory of Medicinal Chemistry, NCI, for FAB-MS data. This research was supported in part by the Intramural Research Program of the NIH, Center for Cancer Research, NCI-Frederick.

**Supporting Information Available:** Spectroscopic data for compounds **7a–j**, synthetic experimental procedures for the acylating species used to synthesize compounds **7j**, and synthetic procedures for mimetics A and B, as well as details of the docking protocol used to generate Figure 1 and procedures for Biacore binding analysis. This material is available free of charge via the Internet at <http://pubs.acs.org>.

## References

- (1) Burke, T. R., Jr. Development of Grb2 SH2 domain signaling antagonists: A potential new class of antiproliferative agents. *Int. J. Pept. Res. Ther.* **2006**, *12*, 33–48.
- (2) (a) Garcia-Echeverria, C.; Gay, B.; Rahuel, J.; Furet, P. Mapping the X+1 binding site of the Grb2-SH2 domain with  $\alpha,\alpha$ -disubstituted cyclic  $\alpha$ -amino acids. *Bioorg. Med. Chem. Lett.* **1999**, *9*, 2915–2920.

- (b) Furet, P.; Gay, B.; Caravatti, G.; Garcia-Echeverria, C.; Rahuel, J.; Schoepfer, J.; Fretz, H. Structure-based design and synthesis of high affinity tripeptide ligands of the Grb2-SH2 domain. *J. Med. Chem.* **1998**, *41*, 3442–3449.
- (3) Oishi, S.; Karki, R. G.; Kang, S.-U.; Wang, X.; Worthy, K. M.; Bindu, L. K.; Nicklaus, M. C.; Fisher, R. J.; Burke, T. R., Jr. Design and synthesis of conformationally constrained Grb2 SH2 domain binding peptides employing  $\alpha$ -methylphenylalanyl based phosphotyrosyl mimetics. *J. Med. Chem.* **2005**, *48*, 764–772.
- (4) (a) Eck, M. J.; Shoelson, S. E.; Harrison, S. C. Recognition of a high-affinity phosphotyrosyl peptide by the Src homology-2 domain of P56(lck). *Nature* **1993**, *362*, 87–91. (b) Waksmann, G.; Shoelson, S. E.; Pant, N.; Cowburn, D.; Kuriyan, J. Binding of a high affinity phosphotyrosyl peptide to the Src SH2 domain: Crystal structures of the complexed and peptide-free forms. *Cell* **1993**, *72*, 779–790.
- (5) Wei, C.-Q.; Li, B.; Guo, R.; Yang, D.; Burke, T. R., Jr. Development of a phosphatase-stable phosphotyrosyl mimetic suitably protected for the synthesis of high affinity Grb2 SH2 domain-binding ligands. *Bioorg. Med. Chem. Lett.* **2002**, *12*, 2781–2784.
- (6) Wysong, C. L.; Yokum, T. S.; McLaughlin, M. L.; Hammer, R. P. 4-Aminopiperidine-4-carboxylic acid: A cyclic  $\alpha,\alpha$ -disubstituted amino acid for preparation of water soluble highly helical peptides. *J. Org. Chem.* **1996**, *61*, 7650–7651.
- (7) Yao, Z. J.; King, C. R.; Cao, T.; Kelley, J.; Milne, G. W. A.; Voigt, J. H.; Burke, T. R. Potent inhibition of Grb2 SH2 domain binding by non-phosphate-containing ligands. *J. Med. Chem.* **1999**, *42*, 25–35.
- (8) Available from Pharmcore Inc., High Point, NC.
- (9) Oishi, S.; Karki, R. G.; Shi, Z.-D.; Worthy, K. M.; Bindu, L.; Chertov, O.; Esposito, D.; Frank, P.; Gillette, W. K.; Maderia, M. A.; Hartley, J.; Nicklaus, M. C.; Barchi, J. J., Jr.; Fisher, R. J.; Burke, T. R., Jr. Evaluation of macrocyclic Grb2 SH2 domain-binding peptide mimetics prepared by ring-closing metathesis of C-terminal allylglycines with an N-terminal  $\beta$ -vinyl-substituted phosphotyrosyl mimetic. *Bioorg. Med. Chem.* **2005**, *13*, 2431–2438.
- (10) (a) Nioche, P.; Liu, W.-Q.; Broutin, I.; Charbonnier, F.; Latreille, M.-T.; Vidal, M.; Roques, B.; Garbay, C.; Ducruix, A. Crystal structures of the SH2 domain of Grb2: Highlight on the binding of a new high-affinity inhibitor. *J. Mol. Biol.* **2002**, *315*, 1167–1177. (b) Liu, W. Q.; Vidal, M.; Gresh, N.; Rogues, B. P.; Garbay, C. Small peptides containing phosphotyrosine and adjacent  $\alpha$ -Me-phosphotyrosine or its mimetics as highly potent inhibitors of Grb2 SH2 domain. *J. Med. Chem.* **1999**, *42*, 3737–3741. (c) Liu, W.-Q.; Vidal, M.; Olszowy, C.; Million, E.; Lenoir, C.; Dhotel, H.; Garbay, C. Structure–activity relationships of small phosphopeptides, inhibitors of Grb2 SH2 domain, and their prodrugs. *J. Med. Chem.* **2004**, *47*, 1223–1233.
- (11) Synthetic procedures for the preparation of mimetics A and B are provided in the Supporting Information.
- (12) Markgren, P. O.; Schaal, W.; Hamalainen, M.; Karlen, A.; Hallger, A.; Samuelsson, B.; Danielson, U. H. Relationships between structure and interaction kinetics for HIV-1 protease inhibitors. *J. Med. Chem.* **2002**, *45*, 5430–5439.

JM0614073